Impact and Detonation of COMP-B An Example using the LS-DYNA® EOS: Ignition and Growth of Reaction in High Explosives

Leonard E Schwer
Schwer Engineering & Consulting Services, Windsor, CA USA

Abstract

*The LS-DYNA keyword *EOS_IGNITION_AND_GROWTH_OF_REACTION_IN_HE provides the ability to model the ignition and growth of the reaction in high explosives via shock initiation from an impact or donor explosive.*

In this preliminary assessment effort, the experimental results for projectile impact on COMP-B of Almond and Murray (2006) are simulated. In addition to reporting their experimental results, the authors also reported numerical simulations results. Further, Urtiew et al. (2006) reported numerical simulation results for this set of experiments, using the same ignition and growth of the reaction in high explosives equation of state, Lee and Traver (1980,) implemented in LS-DYNA, but using a different explicit hydrocode.

The experiments reported by Almond & Murray were for a blunt brass projectile impacting COMP-B without and with cover plates made from steel, aluminum and high density polyethylene. The critical impact speeds were in the range 950 to 1350 meters/second (2000 to 3000 miles/hour). Their numerical simulations used AUTODYN with the Lee and Tarver ignition and growth model.

Similar experiments are reported by Lawrence et al. (2002 and 2006) which also included impact of COMP-B with steel cover plates by projectiles. This series of experiments considered different cover plate thicknesses, projectile nose shapes, and impact obliquity of the projectile. Critical impact speeds ranged from about 1050 to 1600 meters/second for the normal impact cases. The experimental configurations were simulated using the CTH (Hertel et al., 1993) code with the History Variable Reactive Burn (HVRB) explosive initiation model (Kerley, 1995). These experiments are not simulated in the present manuscript, but recommend to interested readers.

In this manuscript the ignition and growth of the reaction in high explosives equation-of-state is introduced along with model parameters for COMP-B. Some comments are included in this section concerning alternative versions of these model parameters that are available in the literature. The manuscript focuses on the experimental data of Almond and Murray, their simulations results, the simulations results of Urtiew et al. and the present results, which make use of the relatively new LS-DYNA axisymmetric Multi-Material Arbitrary Eulerian Lagrange (MM-ALE) capability and thus serve as a post-test form of model validation.

LS-DYNA Keyword: *EOS_IGNITION_AND_GROWTH_OF_REACTION_IN_HE

The interested reader is urged to review the numerous Lawrence Livermore National Laboratory reports describing the development and calibration of this rather complex model. The brief explanation provided here is based on the work of Garcia and Tarver (2006) and the LS-DYNA User Manual sections on the keywords"

*EOS_IGNITION_AND_GROWTH_OF_REACTION_IN_HE
*EOS_PROPELLANT_DEFLAGRATION,

the latter providing a better description of the input parameters shared in common by the two EOS.

As explained by Garcia and Tarver, the basis of the model is two Jones-Wilkins-Lee (JWL) equations-of-state: one representing the detonation products (reacted explosive) and the other representing the unreacted explosive. The general form of the JWL EOS is given by

$$P = Ae^{-R_1 V} + Be^{-R_2 V} + \omega C_V \frac{T}{V}$$

where P is the pressure, V is the relative volume, T is the temperature, ω is the Gruneisen coefficient, C_V is the average heat capacity, A, B, R_1 and R_2 are calibration constants.

The other major component of the model is the reaction rate law for evolving the fraction F of unreacted explosive into detonation products. The reaction rate law has three parts and each is active for different values of the reacted fraction. This three-term rate law describes the three stages of reaction generally observed in shock initiation and detonation of heterogeneous solid explosives.

$$\begin{aligned} \frac{dF}{dt} = I\left[1-F\right]^b \left[\frac{\rho}{\rho_0} - 1 - a\right]^x \quad & \left\{0 < F < F_{ig\max}\right\} \\ + G_1\left[1-F\right]^c F^d P^y \quad & \left\{0 < F < F_{G1\max}\right\} \\ + G_2\left[1-F\right]^e F^g P^z \quad & \left\{F_{G2\min} < F < 1\right\} \end{aligned}$$

Where t is time, ρ is the current density, ρ_0 is the initial density, and I, G_1, G_2, a, b, c, d, e, g, x, y and z are calibration constants.

Urtiew et al. (2006) provide the calibration constants for COMP-B in their Table 4, reproduced here with corrections provided by Traver (2011) for the reader's convenience as Table 1.

Table 1 Ignition & Growth parameters for COMP-B

UNREACTED JWL	REACTED JWL
A=485 Mbar	A=5.242 Mbar
B=-0.0390925 Mbar	B=0.07678 Mbar
$R_1 = 11.3$	$R_1 = 4.2$
$R_2 = 1.13$	$R_2 = 1.1$
$\omega = 0.8938$	$\omega = 0.5$
$C_V = 2.487\times10^{-5}$ Mbar/°K	$C_V = 1.0\times10^{-5}$ Mbar/°K
$T_0 = 298°K$	$E_0 = 0.085$ Mbar
REACTION RATES	
a=0.0367	x=7.0
b=0.667	y=2
c=0.667	z=3.0
d=0.333	$F_{ig\max} = 0.022$

e=0.222	$F_{G1\max} = 0.7$
g=1.0	$F_{G2\min} = 0.0$
$I = 40\ \mu s^{-1}$	$G_1 = 140\ \text{Mbar}^{-2}\mu s^{-1}$
	$G_2 = 1000\ \text{Mbar}^{-3}\mu s^{-1}$
ELASTO-PLASTIC	
$\rho_0 = 1.717\ \text{g/cm}^3$	$G = 0.0354$ Mbar
Yield=0.002 Mbar	

The highlighted parameters in Table 1 are those that differ from the Table 4 in Urtiew et al. The Unreacted JWL parameters A and B were revised in the final version of their paper. The B value provided in the final paper was B=-0.039084 Mbar, but needed to be adjusted for the LS-DYNA implementation to provide a small negative initial pressure in the unreacted explosive. The values for I and G_2 in Table 1 represent corrections to the units that were incorrectly used in the final paper.

Note: Another reference for Lee and Traver ignition and growth COMP-B parameters is the report by Murphy et al. (1993) which lists two sets parameters for what are termed "LANL COMP-B" and "Military COMP-B".

The LS-DYNA manual recommends using *MAT_ELASTIC_PLASTIC_HYDRO (MAT010) with the *EOS_IGNITION_AND_GROWTH_OF_REACTION_IN_HE when the initial pressure is relatively low, i.e. less than 2 to 3 GPa, and the use of *MAT_NULL (MAT009) for higher initial pressures.

The LS-DYNA keyword parameters for the elasto-plastic portion of the model follow:

```
*MAT_Elastic_Plastic_Hydro
$      MID        RO         G       SIGY         EH         PC         FS      CHARL
        15  1.717E-3    3.54E3       20.0
$     EPS1       EPS2       EPS3       EPS4       EPS5       EPS6       EPS7       EPS8

$     EPS9      EPS10      EPS11      EPS12      EPS13      EPS14      EPS15      EPS16

$      ES1        ES2        ES3        ES4        ES5        ES6        ES7        ES8

$      ES9       ES10       ES11       ES12       ES13       ES14       ES15       ES16

$
```

The ignition and growth portion of the model is defined by the following keyword parameters:

```
*EOS_Ignition_and_Growth_of_Reaction_in_HE
$     EOSID          A          B        XP1        XP2       FRER          G         R1
       1507    524.2E3    7.678E3        4.2        1.1      0.667       0.34     48.5E6
$       R2         R3         R5         R6      FMXIG       FREQ      GROW1         EM
-3.90925E3      2.223       11.3       1.13      0.022     40.0E3   14.0E-6        2.0
$       AR1        ES1        CVP        CVR      EETAL      CCRIT        ENQ       TMP0
      0.333      0.667        1.0      2.487        7.0     0.0367      8.5E3      298.0
$     GROW2        AR2        ES2         EN      FMXGR      FMNGR
     1.0E-9        1.0      0.222        3.0        0.7        0.0
```

The above two keyword parameter definitions make use of the consistent metric unit system of grams, millimeters and milliseconds with a derived stress unit of MPa. Also, some nomenclature translation of the ignition and growth keyword parameters to the parameters provided in the above JWL and burn rate equations is required, see Table 2.

Table 2 Keyword parameters to JWL and burn rate equation parameters translation.

UNREACTED JWL	REACTED JWL
R1=A	A=A
R2=B	B=B
R5 = R_1	XP1 = R_1,
R6= R_2	XP2 = R_2
R3= ωC_V	G= ωC_V
TMP0 = T_0	ENQ = E_0
REACTION RATES	
CCRIT=a	EETAL=x
FRER=b	EM=y
ES1=c	EN=z
AR1=d	FMXIG = $F_{ig\max}$
ES2=e	FMXGR = $F_{g1\max}$
AR2=g	FMNGR = $F_{g2\min}$
$I = 4\times10^6\ \mu s^{-1}$	$G_1 = 140\ \text{Mbar}^{-2}\mu s^{-1}$
	$G_2 = 1000\ \text{Mbar}^{-2}\mu s^{-1}$
FREQ = I	GROW1 = G_1
	GROW2 = G_2

Note: The input value for G = ωC_V is 0.34 MPa/K as recommend by Traver, which is not equal to the product of $\omega = 0.5$ and $C_V = 1$ MPa/K as provided in Table 1.

Post-processing of the ignition and growth results includes eight additional history variables, added to the LS-DYNA output data via the keyword *DATABASE_EXTENT_BINARY and its parameters NEIPH or NEIPS, for solids or shells, respectively. The eight history variables were identified by Nicolas Aquelet of LSTC (2011) as

History Variable 1 Temperature,

History Variable 2 $\frac{dE}{dV}$ at fixed F and t with pressure equilibrium,

History Variable 3 C_V heat capacity,

History Variable 4 F fraction (by mass) of high explosive burned,

History Variable 5 $\beta = (1-F)\frac{V_e}{V}$ relative volume fraction of unreacted explosive,

History Variable 6 $\frac{1}{V_e}$ inverse of unreacted explosive relative volume,

History Variable 7 $\frac{1}{V_p}$ inverse of reacted explosive relative volume,

History Variable 8 ρC^2 dynamic pressure(?).

Almond and Murray Experiments and Simulations

In this section the experimental results of Almond & Murray (2005 and 2006) for projectile impacted cylinders of COMP-B are presented. The authors also provide corresponding simulation results which are included in this section. The corresponding simulation results from Urtiew et al. (2006) and the present simulation results are also compared.

The Almond & Murray experiments (2005) focused on simulated land mines impacted by a 50 caliber (12.55 mm diameter) brass blunt projectile. The projectile mass is given as 24 grams, thus for a brass density of 8.53×10^{-3} g/mm^3 this gives an overall projectile length of 22.21 mm. The simulation results of Almond & Murray (2006) use the same projectile but the COMP-B explosive charge is a much smaller cylinder of 40 mm diameter and 30 mm height –

"… sufficient to contain a reaction over the time steps of interest."

i.e. if the COMP-B detonates, it is early on in the impact event, e.g. at about 6 microseconds. The COMP-B charges are either covered by 1 mm steel (1006), 3 mm of aluminum (7039) or 5 mm of high density polyethylene (HDPE). Almond & Murray used AUTODYN and material models from that code's material library. For the three metals, the Johnson-Cook strength model and shock EOS was used with a 250% geo-strain erosion criteria; it is assumed the 'geo-strain' is the effective plastic strain. The authors say the simulations were 2D (assumed to be axisymmetric) although some of the images in their paper appear to be 3D models; see their Figure 3. Further, it is assumed they used the Multi-Material Eulerian feature of AUTODYN. The mesh discretization used was a uniform 0.5 mm mesh, as the authors state there was less than a 3% difference in threshold impact speed when a 0.25 mm mesh was assessed for uncovered (bare) COMP-B.

An overview of the present LS-DYNA axisymmetric Multi-Material ALE (MM-ALE) model of the Almond & Murray experiments is shown in Figure 1. The computational domain is discretized uniformly as square quadrilaterals and the LS-DYNA keyword *INITIAL_VOLUME_FRACTION_GEOMETRY is used to fill the computational domain with the appropriate material, e.g. brass, aluminum, COMP-B and surrounding vacuum. The brass cylinder is given an initial velocity normal to the cover plate. The use of the *INITIAL_VOLUME_FRACTION_GEOMETRY feature makes it simple to refine the mesh, as just the background mesh needs to be redefined. An extensive mesh refinement study was conducted for the bare charge model, and the covered models, using uniform mesh sizes of 0.5, 0.333, 0.25, 0.125 and 0.0625mm. All simulations were performed using ls971_d_Dev_72069_winx64_p.exe.

When the Johnson-Cook strength model is used for the metallic parts, i.e. brass, steel and aluminum, several modeling choices are available for the required equation-of-state (EOS) and also for the optional material failure (erosion). For most engineering work, a simple EOS that

consists of a linear bulk modulus is sufficient. However, for impact speeds in the neighborhood of 1 km/s, it is probably best to use a nonlinear EOS.

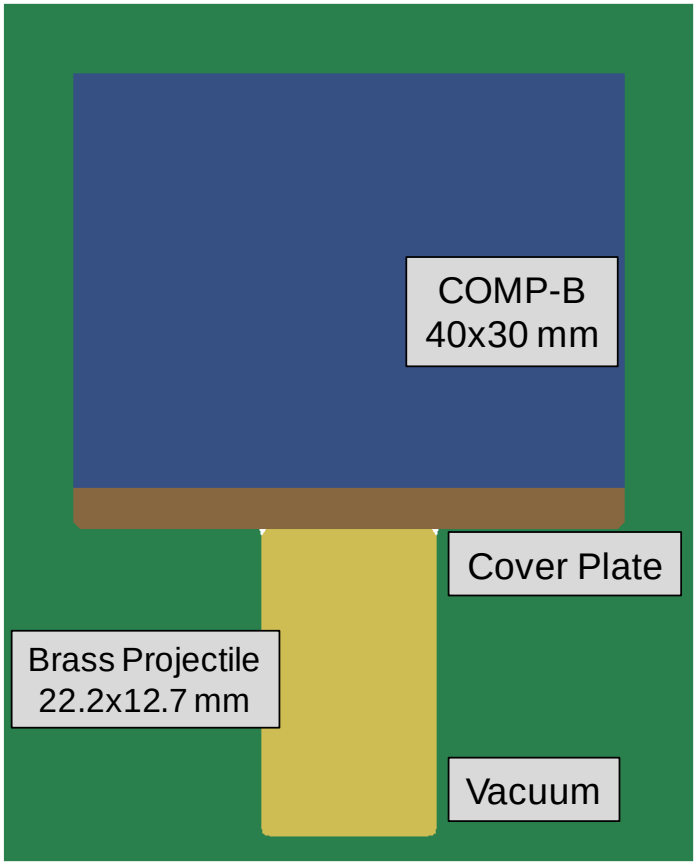

Figure 1 Axisymmetric model for Almond & Murray simulations of brass impactor and COMP-B, shown with 3 mm aluminum cover plate.

Urtiew et al. in their Table 3 provide the Gruneisen equation of state parameters for their three metals and HDPE, reproduced here for the reader's convenience as Table 3. In the numerical results presented by Urtiew et al., only the provided EOS was used for the metals, i.e. no strength model was included.

Table 3 Gruneisen equation of state parameters from Urtiew et al. (2006)

Material	ρ_0 (g/cm^3)	C (mm/μs)	S_1	S_2	S_3	γ_0	a
Al 6061	2.703	5.24	1.4	0.0	0.0	1.97	0.48
Steel	7.90	4.57	1.49	0.0	0.0	1.93	0.5
Brass	8.45	3.834	1.43	0.0	0.0	2.0	0.0
HDPE	0.954	3.0	1.44	0.0	0.0	1.0	0.0

When the Johnson-Cook strength model is used, the user may optionally include the five Johnson-Cook failure parameters, typically denoted D_1 through D_5, impose an ad hoc failure criteria, e.g. 250% geo-strain erosion criterion, or ignore material failure by setting the five

failure parameters to zero. In the present analysis, the five failure parameters were included since they are available from Johnson and Holmquist (1989) for the three metals of interest.

When material failure, or erosion, is invoked, the LS-DYNA MM-ALE user has the option to replace the failed material with either vacuum (default) or another material model. In the present simulations, the failed Johnson-Cook material is replaced by the same material model and Gruneisen equation of state. Since the deviatoric stresses are set to zero by the Johnson-Cook model at failure, the Gruneisen equation of state for pressure provides the only material stress, i.e. the failed material is modeled in the 'no strength' manner used by Urtiew et al. This optional method of replacing the failed material basically amounts to providing a visualization of what material has failed, as the MM-ALE ALE Multi-Material Group (AMMG) ID is different for the original and failed Johnson-Cook material. Optionally, the failed Johnson-Cook material could have been replaced by *MAT_NULL (MAT009), i.e. zero shear strength, but this was thought to be unnecessary. Replacing the failed Johnson-Cook material by vacuum is not recommended as then there is no equation of state generated pressure to resist compression.

Detonation or No Detonation, That is the Question

> "Steady detonation may be considered as a self-propagating process where the effect of compression of the shock front discontinuity changes the state of the explosive so that the exothermic reaction is established with the requisite velocity. The increase in pressure, temperature, and density can occur during a time interval as short as a few picoseconds …" Smith and Hetherington (1994)

When performing impact detonation experiments, e.g. Almond & Murray (2005), it is usually obvious when the explosive detonates, as the chemical energy is rapidly turned into internal energy in the form of visible light, heat and shock waves. However, for numerical simulations there is no visible light, and they typically lack availability of temperature histories, so shock waves serve as an indicator of detonation. Perhaps a better indicator of detonation is the burn fraction history variable, i.e. History Variable 4, associated with the LS-DYNA *EOS_IGNITION_AND_GROWTH_OF_REACTION_IN_HE. When the burn fraction is unity, this is an indication of detonation of the explosive as the explosive has been fully transformed into detonation products. When this burn fraction extends to all of the available explosive, detonation is assumed to have occurred.

The shock wave criterion for detonation used here is pressure exceeding the Chapman-Jouquet pressure, i.e. 29.5 GPa for COMP-B as per Dobratz and Crawford (1985). The Chapman-Jouquet pressure is the point where the Rayleigh Line is tangent to the Hugoniot. At pressures below the Chapman-Jouquet pressure, detonation, or deflagration, may also occur, but above the Chapman-Jouquet pressure only detonation occurs.

The pressure in the COMP-B is monitored at eleven Langrage tracer particles located along the axis of symmetric, and initially spaced 0.3 mm apart. The initial, and T=0.012 ms, location of the tracer particles are shown in Figure 2 with the tracer particle T11 closest to the projectile and tracer particle T1 at the rear surface of the COMP-B explosive. The right side of this figure also illustrates the deformation of the COMP-B, and blunt brass projectile, for an impact speed of 1 km/s, just below the detonation threshold for the 0.333 mm mesh. The green region near the

center of the projectile is the failed brass material as predicted by the Johnson-Cook material model.

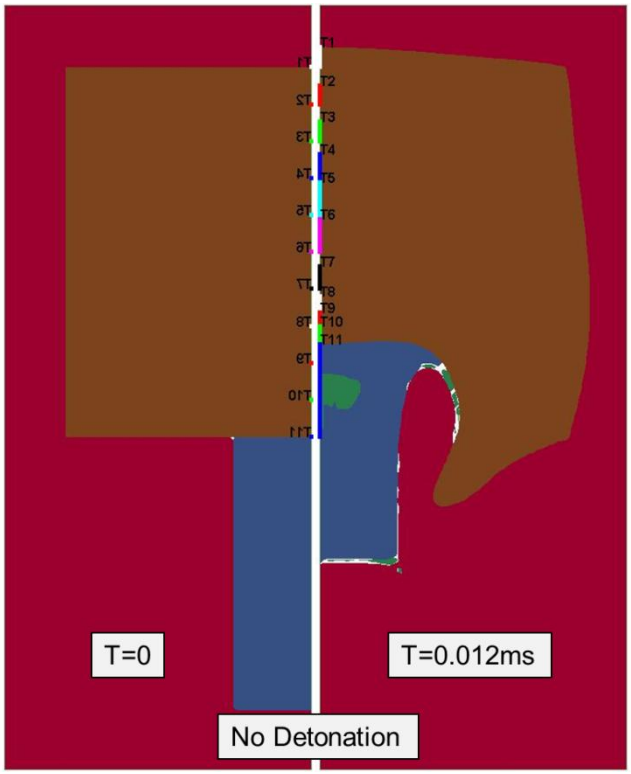

Figure 2 Bare COMP-B explosive with blunt brass impactor showing initial and deformed location of Lagrange Tracer Particles.

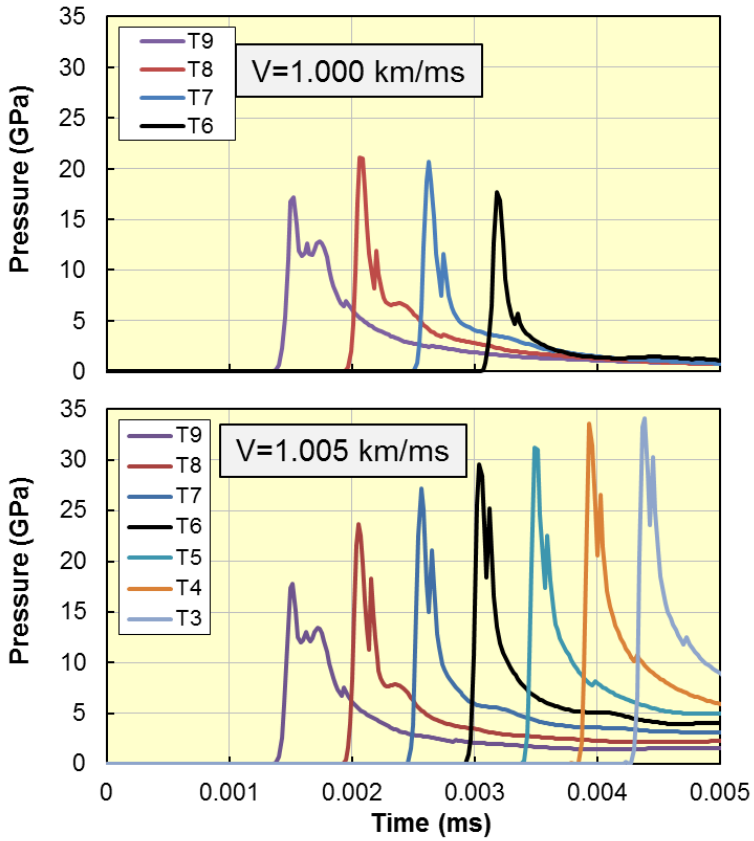

Figure 3 Tracer particle pressure histories for no detonation impact at V=1.000 km/s (upper image) and detonation impact at V=1.005 km/s (lower image).

Figure 3 shows the pressure histories at several tracer locations for the no detonation impact speed of 1.000 km/s (upper image) and detonation of the COMP-B at an impact speed of 1.005 km/s (lower image). Recall the Chapman-Jouquet pressure for COMP-B is about. 29.5 GPa, and none of the tracer locations for the lower speed impact approach this pressure. For the faster impact speed, the maximum pressure increases nearly linearly with distance into the COMP-B, i.e. moving from close to the projectile (T9) to more distant from the impact location (T3). The tracer at T5 is the first tracer to exceed the Chapman-Jouquet pressure.

When detonation occurs, at about 0.006 ms, the stable time step often drops dramatically, i.e. by 2 to 3 orders of magnitude. This large decrease in the time step is due to the stability limit in MM-ALE simulations which requires the minimum time step be less than not only the element characteristic length divide by the sound speed, but rather the length divided by the sound speed plus the particle speed. It is the particle speed that increases dramatically when detonation occurs. With a much reduced stable time step, there is little point is continuing the simulation, since in this study only the 'No-Go' or 'Go' impact speeds are of interest.

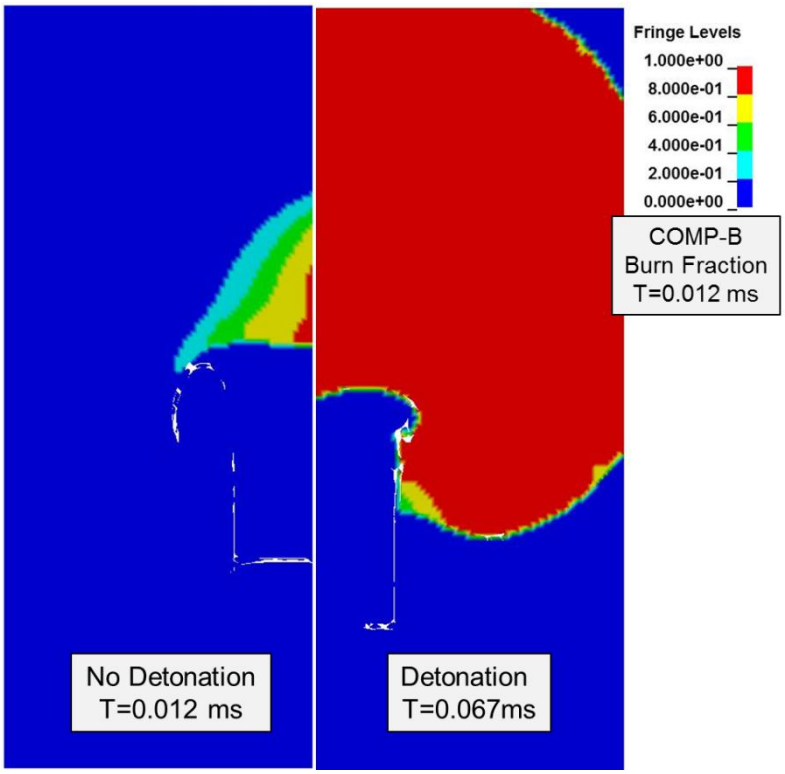

Figure 4 Fringe of burn fraction history variable in the COMP-B for the 1.000 km/s impact (left) and 1.005 km/s impact (right).

Figure 4 shows fringes of the COMP-B burn fraction history variable for an impact speed of 1. 000 km/s (left) were detonation does not occur, and impact at 1.005 km/s (right) where all of the COMP-B has been burned, i.e. detonation of the explosive. Although some of the COMP-B in the lower speed impact appears (red color) as having been burned, the maximum burn fraction is only about 85%.

Bare Charge Mesh Refinement Study

Before presenting the results comparisons, it is always necessary when using the MM-ALE solver to perform mesh refinement (convergence) studies. The initial LS-DYNA mesh size was guided by the work of Almond & Murray (2006):

> "The 0.50 mm square mesh was selected for both projectile and target after preliminary testing with a 0.25 mm mesh produced just 3% difference in the threshold velocity against bare explosive."

This uniform mesh size is significantly larger than the mesh size quoted by Urtiew et al. (2006) who used 50 zones per mm (0.02 mm) for some related one dimension simulations. However, they did not quote a mesh size, nor indicate mesh convergence, for their replication of the Almond & Murray (2006) simulations, only stating

> "…experiments were modeled in finely zoned 2D calculations …"

Table 4 Mesh refinement results for bare COMP-B charge.

Mesh Size (mm)	Number Elements	Δt (ns)	CPU (sec)	No Go (km/s)	Go (km/s)
0.500	6200	0.605	214	0.960	0.965
0.333	13950	0.403	85	1.000	1.005
0.250	24800	0.298	135	1.020	1.025
0.125	99200	0.151	2135	1.060	1.065
0.0625	395409	0.074	27187	1.080	1.085

Table 4 summarizes the mesh refinement results for the bare COMP-B charge impacted by a blunt brass projectile. The time step listed in the third column is the initial time step estimated by LS-DYNA using a TSSFAC=0.6. The CPU time is for the detonation case, i.e. 'Go' impact speed. The difference between the 'No Go' and 'Go' impact speeds was only determined to within a 5 m/s interval, so while the total CPU time to detonation varies primarily with the number of elements and time step size, it also depends on how close the prescribed 'Go' speed was to incipient detonation.

In addition to mesh refinement, LS-DYNA MM-ALE simulations involving explosives should also examine the effect of varying the advection method, i.e. the METH parameter on the *CONTROL_ALE keyword. For this study METH=3 advection option was used:

> "donor cell + HIS, first order accurate, conserving total energy over each advection step instead of conserving internal energy"

Historically, this was the recommend advection method when explosive were explicitly modeled. Recently, METH=-2 (minus 2) option has been added and is now recommended when explosives are modeled:

> "Van Leer + HIS, with the monotonicity condition relaxed during advection process to better preserve *MAT_HIGH_EXPLOSIVE_BURN material interface."

Three of the four advection methods, i.e. METH=2,-2, and 3, were assessed using only the 0.333 mm mesh. Both METH=2 and METH=-2 produced the same 'No Go' and 'Go' impact speeds of 1.010 and 1.015 km/s, respectively. These compare to the METH=3 results, from Table 4, of 1.000 and 1.005 km/s, respectively, for the 'No Go' and 'Go' impact speeds. The recommendation is made to always assess all the advection methods for every MM-ALE modeling task.

When axisymmetric MM-ALE simulations are performed, it is also recommend to assess the two element weighting options, ELFORM, available on the *SECTION_ALE2D. ELFORM=14 uses an area weighting and ELFORM=15 uses a volume weighting. These weighting options have various advantages and disadvantages, however, their difference is usually most pronounced along the axis of symmetry – where typically most of the critical response occurs in such axisymmetric simulations.

Figure 5 summarizes the 'Go' impact speed mesh refinement results for the bare COMP-B charge using both the area (ELFORM=14) and volume (ELFORM=15) options. The mesh sizes ranged from h=0.5 mm (2=1/0.5) to h=0.0625 mm (16=1/0.0625). As can be seen, the area weighted results require a slightly greater impact speed for detonation than the corresponding volume weighted simulations. However, both sets of results have not converged, despite using much finer meshes, e.g. 0.0625 mm, than was observed by Almond & Murray (2006): their 0.5 and 0.25 mm meshes did not indicate a significant difference in critical impact speed. Although the

difference between the area and volume weighted responses seems to decrease with increasing mesh refinement, the lack of convergence at a relatively small mesh sizes bodes ill for more practical three dimensional simulations.

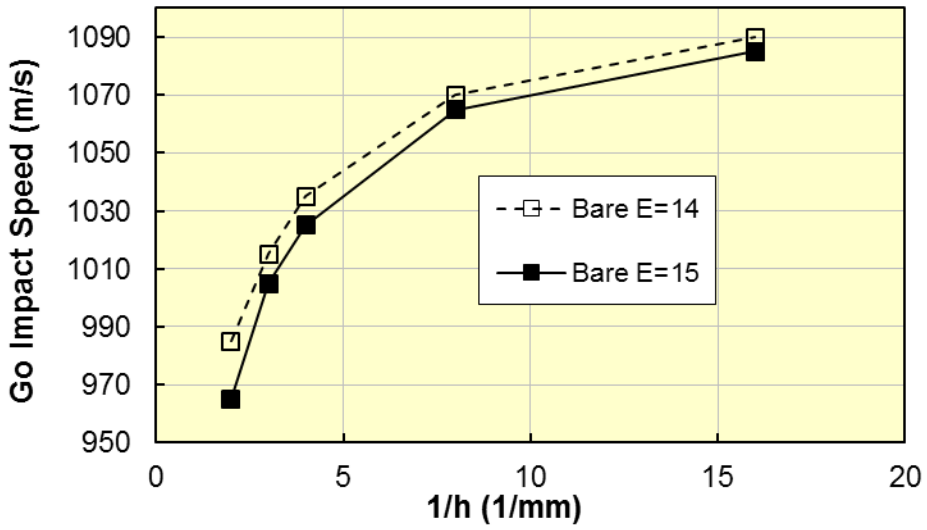

Figure 5 Bare COMP-B 'Go' impact speed mesh convergence results for two forms of element weighting.

Comparison of Results

In this section, comparisons of critical impact speeds as determined by Almond & Murray in their reported mine impact experiments (2005) and small charge AUTODYN simulations (2006) are presented. Also presented are the so called "No-Go" and "Go," i.e. no-detonation and detonation, respectively, impact speeds reported by Urtiew et al. for their simulations of the Almond & Murray calculations Finally, the present LS-DYNA results are compared with the these results

Bare Charge

The recommendation is made for those new to *EOS_IGNITION_AND_GROWTH_OF_REACTION_IN_HE modeling to start with the simplest model possible. Thus eliminating the metal cover plate is an important simplification. Also, the blunt projectile used by Almond & Murray simplifies the mesh and mesh refinement compared to ogival type projectiles which are more common in practical application.

Figure 6 summarizes the critical impact speeds for detonation of the bare COMP-B charge impacted by the blunt brass projectile. The experimental and simulation results reported by Almond & Murray (2006) are 969 and 840 m/s, respectively[1]. Urtiew et al. reported a 'Go" impact speed of 990 m/s[2]. As can be seen, the coarsest LS-DYNA meshes provide impact speeds corresponding to the experiment and the Urtiew et al results. However as noted above, and obvious in this figure, these LS-DYNA results are not converged.

[1] Almond & Murray did not state a speed interval for their experimental, nor numerical, results.
[2] The 'No Go' to 'Go' impact speed interval used by Urtiew et al. was 10 m/s.

Several possibilities exist for explaining these bare COMP-B detonation speed differences:

- The AUTODYN implementation used by Almond & Murray may differ significantly from the present LS-DYNA implementation of an ignition and growth model,
- A similar possible implementation difference exists with the implementation used by Urtiew et al.,
- Perhaps a mesh refinement study, if performed, by Urtiew et al. would also indicate a lack of convergence, recall their mesh size was not stated.
- Almond & Murray did not provide a critical impact speed interval.

Without a mesh refinement study, it is possible to conclude that the course mesh results are 'accurate,' especially if the experimental or other computational results are known. However, typically simulations are performed for the purpose of predicting response. In such cases, omitting mesh convergence studies is hazardous, especially for those depending on the analysis results.

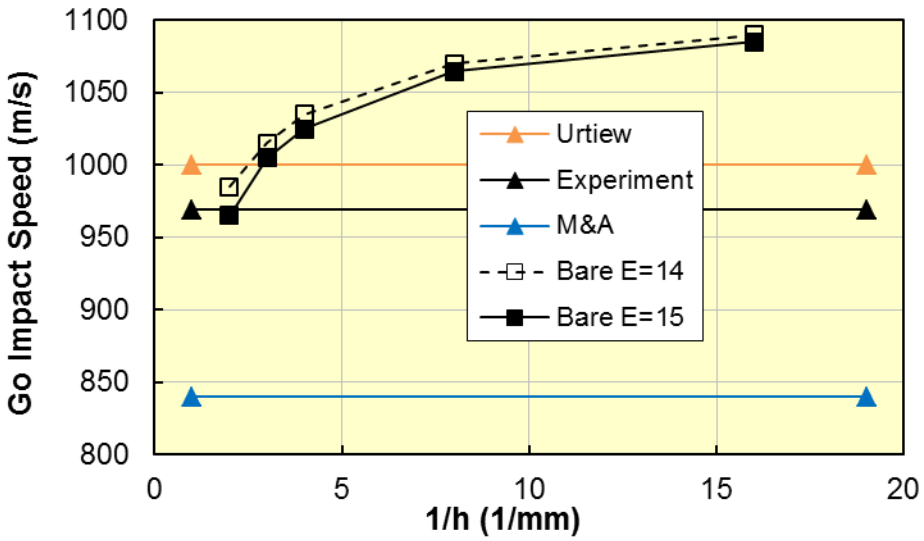

Figure 6 Bare COMP-B detonation impact speed comparisons.

Steel Cover Plate 1 mm Thick

Neither Almond & Murray, nor Urtiew et al., reported the type of steel used for the cover plate in their simulations. Urtiew et al. did provide the equation-of-state parameters they used, refer back to Table 3, and no strength model was included in their simulations. The decision was made to use the available Johnson-Cook parameters from the Los Alamos report (1989) for steel 1006. This will allow others to repeat the present simulations and easily reference the Johnson-Cook model material parameters.

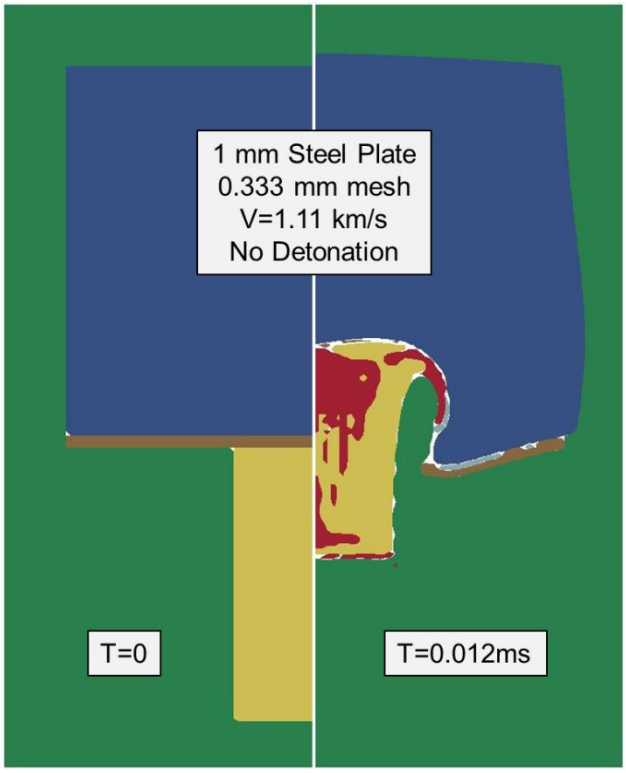

Figure 7 Steel plate covered COMP-B explosive with blunt brass impactor showing initial and deformed configurations for 0.333 mm mesh without detonation.

Figure 7 shows the initial (left) model with the thin 1 mm steel plate and the deformed configuration (right) at the end of the simulation, i.e. T=0.012 ms. Both the brass projectile and thin steel plate have failed regions predicted by the Johnson-Cook model. The failed replacement material is indicated by the changed color for each part. Although the COMP-B explosive has deformed significantly, there is no detonation at 1.11 km/s for the 0.333 mm mesh size displayed.

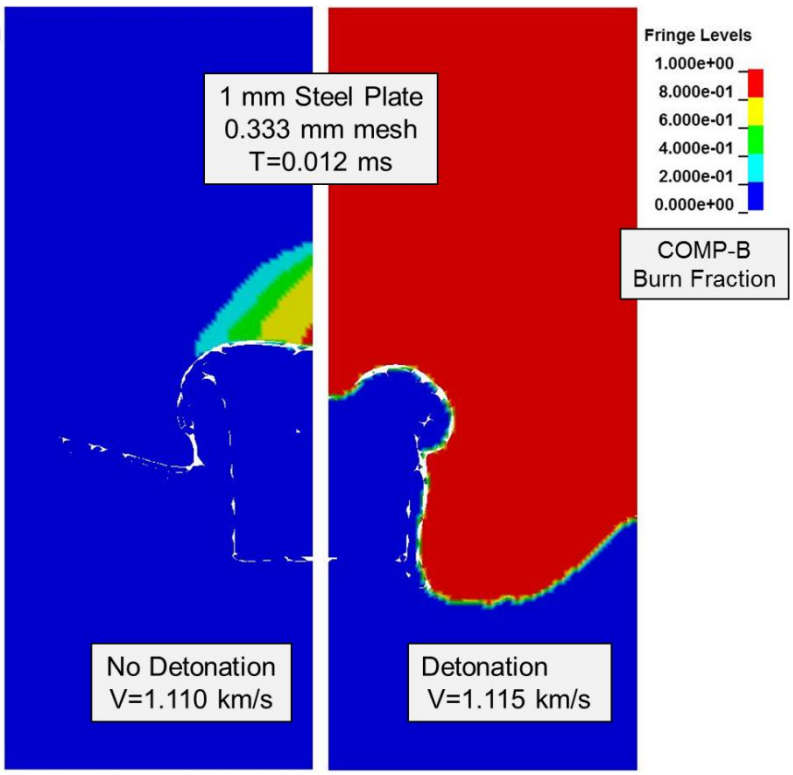

Figure 8 Fringes of the burn fraction history variable in the COMP-B for the 1.110 km/s impact (left) and 1.115 km/s impact (right) steel plate cover 0.333 mm mesh.

Figure 8 shows fringes of the COMP-B burn fraction history variable for an impact speed of 1. 110 km/s (left) were detonation does not occur, and impact at 1.115 km/s (right) where all of the COMP-B has been burned, i.e. detonation of the explosive. Although some of the COMP-B in the lower speed impact appears (red color) as having been burned, the maximum burn fraction is only about 83%.

Figure 9 summarizes the critical impact speeds for detonation of the COMP-B charge covered by 1 mm of steel when impacted by the blunt brass projectile. The experimental and simulation results reported by Almond & Murray (2006) are 1086 and 940 m/s, respectively. Urtiew et al. reported a 'Go" impact speed of 1120 m/s. As can be seen, the coarsest LS-DYNA meshes provide impact speeds corresponding to the experiment and the Urtiew et al results, however as noted previously, these LS-DYNA results are not converged.

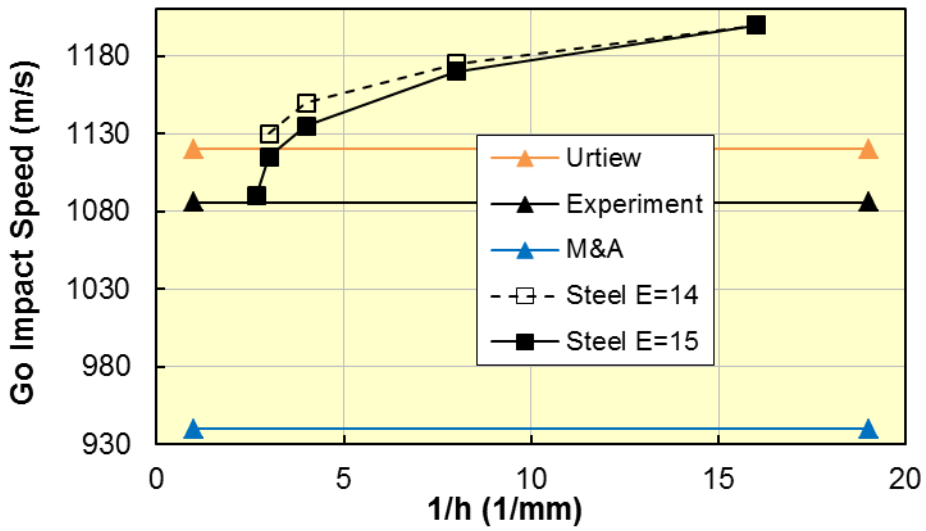

Figure 9 Steel cover plate COMP-B detonation impact speed comparisons.

Aluminum Cover Plate 3 mm Thick

Almond & Murray did report the type of aluminum used for the cover plate in their simulations. Urtiew et al, provided equation of state parameters for aluminum 6061-T6, refer back to Table 3. In the present LS-DYNA simulations, the equation of state parameters provided by Urtiew et al, are used, as this makes for a more direct comparison with their results. Although Urtiew et al. did not use a strength model for the metals in their simulations, the decision was made to use the available Johnson-Cook parameters from the Los Alamos report (1989) for aluminum 7079. This will allow others to repeat the present simulations and easily reference the Johnson-Cook model material parameters.

Figure 10 shows the initial (left) model with the 3 mm aluminum plate and the deformed configuration (right) at the end of the simulation, i.e. T=0.012 ms. Both the brass projectile and thin aluminum plate have failed regions predicted by the Johnson-Cook model. The failed replacement material is indicated by the changed color for each part. Although the COMP-B explosive has deformed significantly, there is no detonation at 1.16 km/s for the 0.333 mm mesh size displayed.

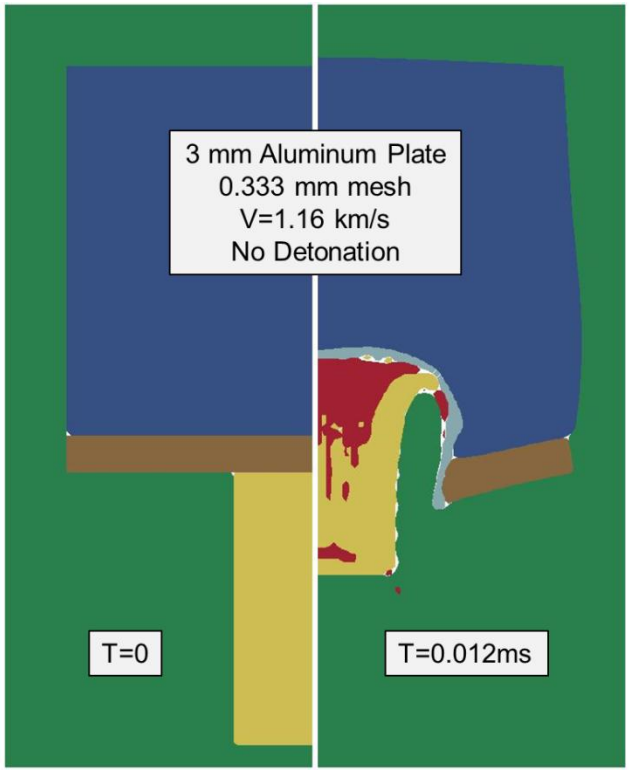

Figure 10 Aluminum plate covered COMP-B explosive with blunt brass impactor showing initial and deformed configurations for 0.333 mm mesh without detonation.

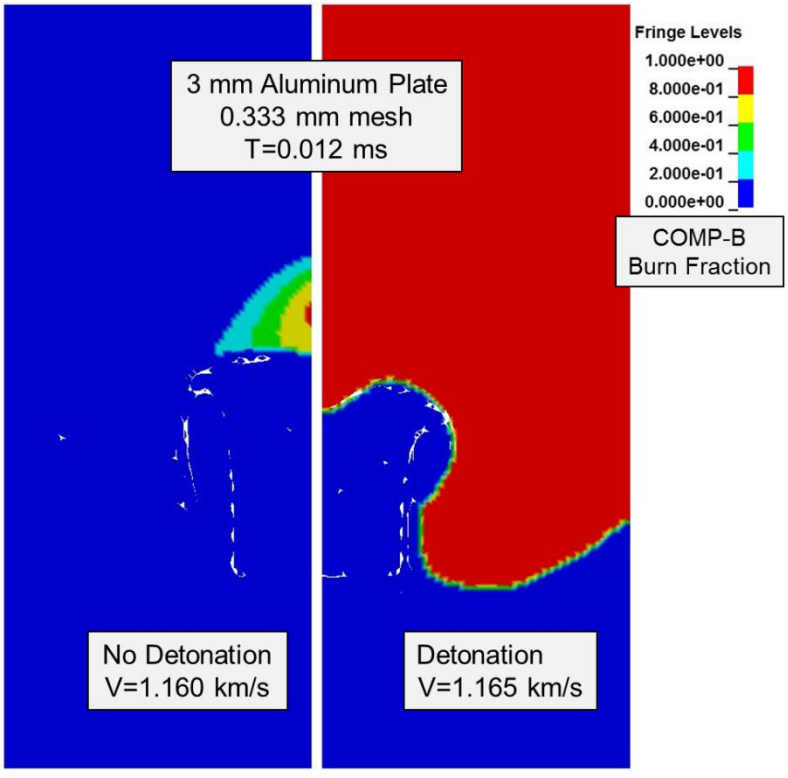

Figure 11 Fringes of the burn fraction history variable in the COMP-B for the 1.160 km/s impact (left) and 1.165 km/s impact (right) aluminum plate cover 0.333 mm mesh.

Figure 11 shows fringes of the COMP-B burn fraction history variable for an impact speed of 1.160 km/s (left) were detonation does not occur, and impact at 1.165 km/s (right) where all of the COMP-B has been burned, i.e. detonation of the explosive. Although some of the COMP-B in the lower speed impact appears (red color) as having been burned, the maximum burn fraction is only about 85%.

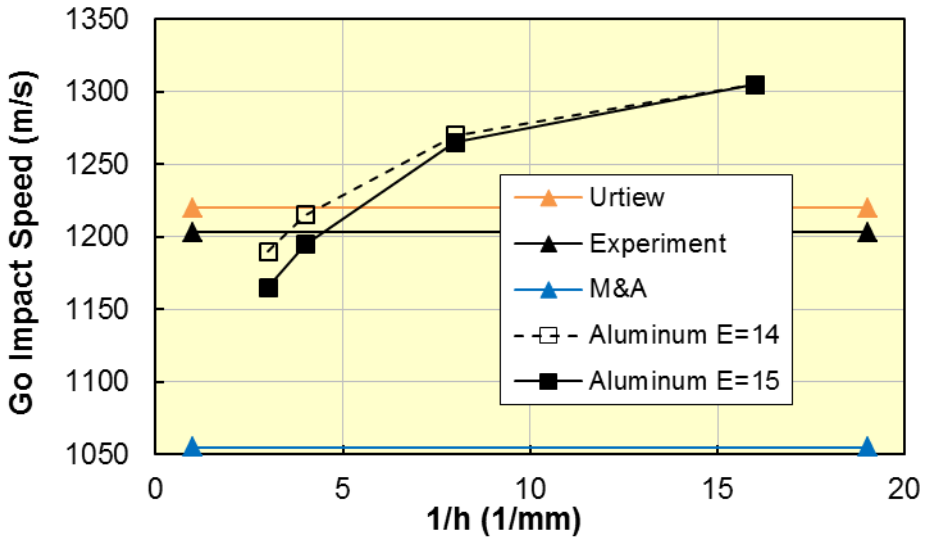

Figure 12 Aluminum cover plate COMP-B detonation impact speed comparisons.

Figure 12 summarizes the critical impact speeds for detonation of the COMP-B charge covered by 3 mm of aluminum when impacted by the blunt brass projectile. The experimental and simulation results reported by Almond & Murray (2006) are 1203 and 1055 m/s, respectively. Urtiew et al. reported a 'Go" impact speed of 1220 m/s. As can be seen, the 0.25 mm (4=1/0.25) LS-DYNA mesh provides impact speeds corresponding to the experiment and the Urtiew et al results, however as noted previously, and obvious again in this figure, these LS-DYNA results are not converged.

Summary

The experiments and numerical results reported by Almond & Murray provide an attractive starting point for investigation of the LS-DYNA *EOS_IGNITION_AND_GROWTH_OF_REACTION_IN_HE model, since the bare charge configuration simplifies the model and required material data. Additionally, the blunt projectile geometry also simplifies the mesh, and especially the mesh refinement.

The experiments and simulations reported by Almond & Murray (2006) of a blunt brass projectile impacting COMP-B charges without and with metal cover plates have been simulated using then LS-DYNA keyword *EOS_IGNITION_AND_GROWTH_OF_REACTION_IN_HE. In general, the coarse mesh 0.333 mm results agree fairly well with their experimental results, and the corresponding simulation results reported by Urtiew et al. (2006). However, mesh refinement studies with the present LS-DYNA model indicate significantly greater projectile impact speeds are required to detonate the COMP-B as the mesh is refined. It appears the critical impact speed

will converge for mesh sizes smaller than 0.0625 mm, although no mesh smaller than 0.0625 was attempted in the present study.

In addition to mesh refinement, a comparison between the two types of axisymmetric weighting options, i.e. area and volume, were examined for all mesh sizes studied. The area weighting option requires a slightly greater impact speed to detonate the explosive than for the corresponding volume weight case. However, as the mesh is refined, the critical impact speed difference between these two options decreases.

For the bare COMP-B charge, a small sensitivity study was performed with the coarse 0.333 mm mesh of three of the four available LS-DYNA advection methods. Two of the three advection options, i.e. METH=2 and -2, provided the same critical impact speed. The third advection option, METH=3, required a slight greater impact speed to detonate the COMP-B. The current user manual recommendation appears to be the use METH=-2 when explosives are explicitly modeled using the MM-ALE solver.

Acknowledgements

A deep debt of gratitude is owed to Craig Tarver for numerous discussions, his patience, and expert guidance that made this manuscript possible. Thanks too to Bence Gerber for guidance on AUTODYN equation-of-state and Johnson-Cook material model library data and Nicolas Aquelet for his help with the associated history variables and many much appreciated discussions on the mysteries of the LS-DYNA MM-ALE implementation.

References

Almond RJ and SG Murray, "Projectile Attack of Surface Scattered Munitions Comparing Closed Form Theory with Live Trials," Propellants, Explosives, Pyrotechnics, Volume 30, Number 3, (2005)

Almond, RJ and SG Murray, "Projectile Attack of Surface Scattered Munitions: Prompt Shock Finite Element Models and Live Trials," Propellants, Explosives, Pyrotechnics, Volume 31, Number 2, (2006)

Aquelet, N., personal communication via email on 3 February 2011.

Dobratz, BM and PC Crawford, "LLNL explosives handbook: properties of chemical explosive and explosive stimulants," Lawrence Livermore National Laboratory, University of California, 1985.

Garcia, ML and CM Tarver, "Three-Dimensional Ignition and Growth Reactive Flow Modeling of Prism Failure Tests on PBX 9502," 13th International Detonation Symposium Norfolk, VA, United States July 23, 2006 through July 28, 2006. (UCRL-CONF-222376)

Hertel, ES. Jr, RL. Bell, MG. Elrick, AV. Farnsworth, GI. Kerley, JM. McGlaun, SV Petney, SA Silling, PA Taylor, and L Yarrington. "CTH: A Software Family for Multi-Dimensional Shock Physics Analysis." Proceedings of the 19th International Symposium on Shock Waves, Volume 1, Pages 377-382, July 1993.

Hetherington JG and PD Smith, "Blast and Ballistic Loading of Structures" Publisher: Laxton's (November 15, 1994) ISBN-10: 0750620242 ISBN-13: 978-0750620246.

Johnson, GR, and TJ Holmquist, "Test Data and Computational Strength and Fracture Model Constants for 23 materials Subjected to Large Strains, High Strain Rates, and High Temperatures," Los Alamos Technical Report LA-11463-MS, Los Alamos National Laboratory, Los Alamos, NM, 1989.

Kerley, G. I. "CTH Equation of State Package: Porosity and Reactive Burn Models." SAND92-0553, Sandia National Laboratories, Albuquerque NM, April 1995.

Lawrence, W., Krzewinski, B., Starkenberg, J., and Baker, P., "Projectile-Impact Shock-Initiation Experiments and CTH Simulation Comparisons," Army Research Laboratory Report ARL-RP-116, Aberdeen Proving Ground, MD, February 2002.
(Proceedings of the JANNAF Propulsion Systems Hazards Subcommittee Meeting, Destin, FL, April 2002.)

Lawrence, W., and Starkenberg, J., "Effects of Projectile and Cover Material Strength and Projectile Shape on the Impact Initiation of Composition B," HPCMP Users Group Conference, 2006, Pages 106-109, June 2006 (ISBN: 0-7695-2797-3)

Lee, E.L. and C.M. Tarver, "Phenomenological Model of Shock Initiation in Heterogeneous Explosives," Phys. Fluids 1980, 23(12),2362.

Murphy, M.J., E.L. Lee, A.M. Weston, and A.E. Williams, "Modelling Shock Initiation in Composition B," 10th Symposium (International) on Detonation, Boston, MA, July 11 – 16, page 148, 1993 (UCRL-JC-111975)

Traver, C., personal communication via series of emails, January – March 2011.

Urtiew, PA, KS Vandersall, CM. Tarver, F Garcia, and JW Forbes, "Shock Initiation Experiments and Modeling of Composition B and C-4," 13th International Detonation Symposium Norfolk, VA, United States July 23, 2006 through July 28, 2006. (UCRL-CONF-222137)